SUPPLEMENTAL MATERIAL

SUPPLEMENTAL FIGURES

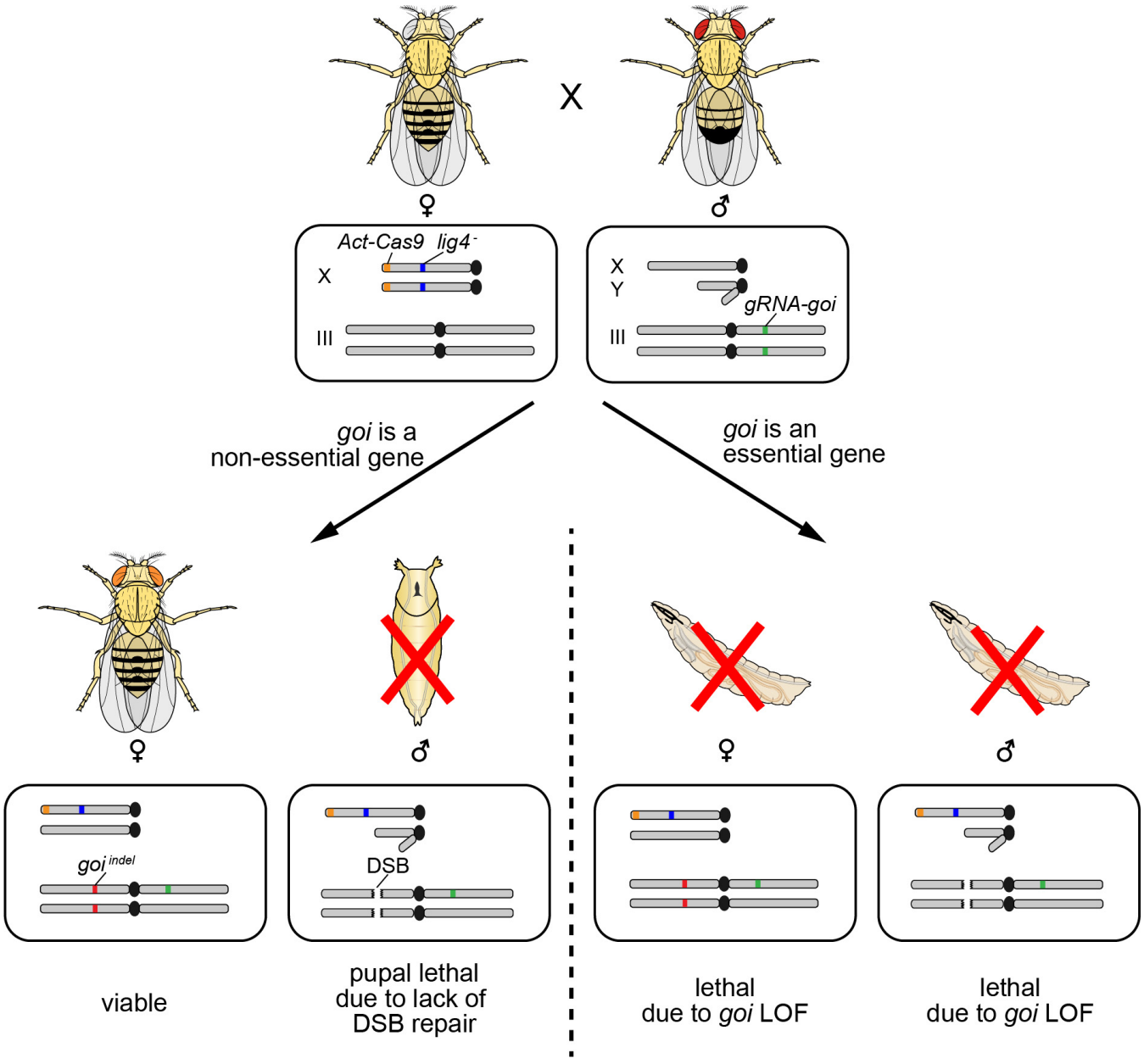

Figure S1. Cas9-LEThAL assay.

In Cas9-LEThAL (for Cas9-induced lethal effect through the absence of Lig4) assay, homozygous males of gRNA for *goi* (a hypothetic gene name for *gene of interest*, which is on the third chromosome in the illustrated example) are crossed to *Act-Cas9 lig4* homozygous females. As *Act-Cas9* and the *lig4* null mutation are both on the X chromosome, the male progeny from the cross is *lig4* deficient and therefore cannot repair DNA double-stranded breaks (DSBs) through NHEJ. In contrast, the female progeny is

heterozygous for *lig4* and thus can repair DSBs. Efficient gRNAs will target the *goi* locus to create bi-allelic DSBs, which will be repaired to generate indels in female somatic cells but left unrepaired in male somatic cells. If *goi* is a non-essential gene, female progeny with indel mutations at the *goi* locus should be viable while male progeny will die from late third instar to the pupal stage due to the lack of DSB repair. The lack of lethality at earlier stages in the male progeny may be explained by mechanisms that facilitate proper segregation of chromatid fragments into daughter cells during mitosis (ROYOU *et al.* 2010). If *goi* is an essential gene, *goi* LOF will cause both female and male progeny to die to at a stage similar to the lethal phase of *goi* zygotic null mutants. Viable male progeny from this cross indicates inefficient gRNAs. All flies in this assay carry a *w* mutation, which is omitted from the diagram.

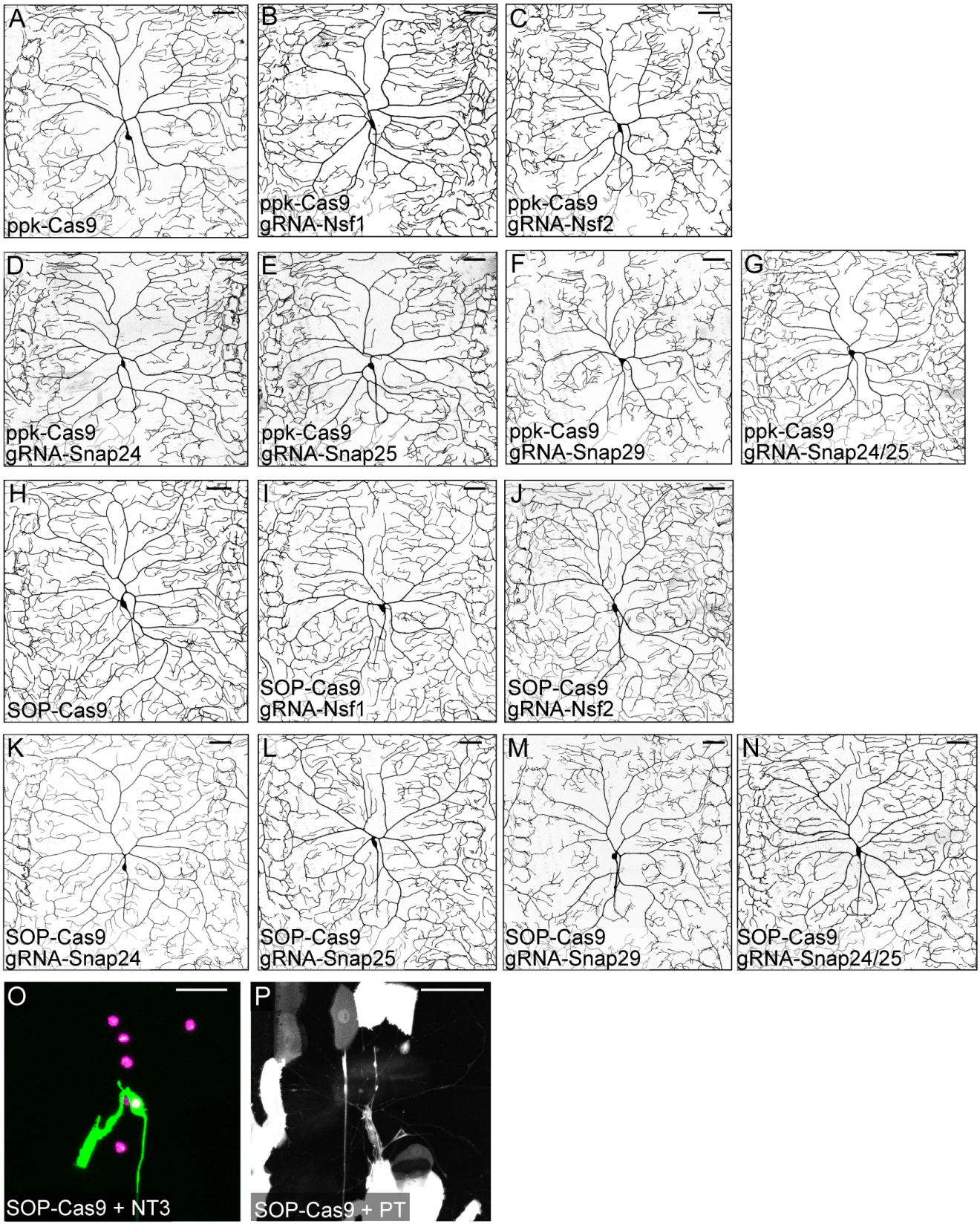

Figure S2. LOF of individual NSF and SNAP genes in C4da neurons.

(A-G) DdaC neurons in the *ppk-Cas9* control (A), *ppk-Cas9 gRNA-Nsf1* (B), *ppk-Cas9 gRNA-Nsf2* (C), *ppk-Cas9 gRNA-Snap24* (D), *ppk-Cas9 gRNA-Snap25* (E), *ppk-Cas9 gRNA-Snap29* (F), and *ppk-Cas9 gRNA-Snap24-Snap25* (G). (H-N) DdaC neurons in the *SOP-Cas9* control (H), *SOP-Cas9 gRNA-Nsf1*(I), *SOP-Cas9 gRNA-Nsf2* (J), *SOP-Cas9 gRNA-Snap24* (K), *SOP-Cas9 gRNA-Snap25* (L), *SOP-Cas9 gRNA-Snap29* (M), and *SOP-Cas9 gRNA-Snap24-Snap25* (N). (O and P) Cas9 activity patterns of *SOP-Cas9* with the negative tester NT3 (O) and the positive tester (PT) and (P). (Scale bars, 50 μm).

Table S1. List of positive and negative tester lines.

Tester	Genotype	Comment
Positive Tester (PT)	*Act-Gal4 UAS-GFP; tub-Gal80 gRNA-Gal80*	ubiquitous tester*
Negative Tester 1 (NT1)	*gRNA-GFP UAS-mCherryNLS; Act-Gal4 UAS-GFP*	ubiquitous tester**
Negative Tester 2 (NT2)	*gRNA-GFP UAS-mCherryNLS; tubP-Gal4 UAS-CD8-GFP*	ubiquitous tester
Negative Tester 3 (NT3)	*21-7 UAS-CD4-tdGFP; gRNA-GFP UAS-RedStinger*	PNS tester
Negative Tester 4 (NT4)	*gRNA-GFP UAS-mCherryNLS; nsyb-Gal4 UAS-CD4-tdGFP*	pan-neuronal tester

* PT shows Cas9-independent expression in the gut.

** The Gal4 is not active in imaginal discs.

Table S2. Results of the Cas9-LEThAL assay.

Gene Name	Cas9-LEThAL assay lethal phase	Reported lethal phase of null mutants
e	Males: prepupae; females: viable	viable
Ptp69D	Pharate adults	Pupae with rare escapers (DESAI AND PURDY 2003)
Nsf1 (*comt*)	Males: early pupae; female: pharate adults to newly eclosed adults (dead in the food)	Late pupae (pharate adults) (GOLBY *et al.* 2001)
Nsf2	1st instar larvae	1st instar larvae (GOLBY *et al.* 2001)
Nsf1/Nsf2	1st instar larvae	unknown
Snap24	2nd instar larvae to early 3rd instar larvae	unknown
Snap25	Males: early pupae; females: pharate adults	Late pupae (pharate adults) (VILINSKY *et al.* 2002)
Snap29	1st instar larvae to early 3rd instar larvae	Early larvae (MORELLI *et al.* 2014)
Snap24/Snap25	1st instar larvae	unknown
Snap24/Snap25/Snap29	Late embryos to early 1st instar larvae	unknown

Table S3. List of gRNA construct and target sequences.

gRNA lines	gRNA cloning vector	gRNA target sequences
gRNA-Gal80	pAC-U61-SapI	1: GATAGTGATAGCTATCCAAG 2: AACAAGCTCCTTTAGACCCG
gRNA-GFP	pAC-U61-SapI pAC-U61-SapI-Rev pAC-U61-SapI-In pAC-U63-tgRNA-Rev	1: CAACTACAAGACCCGCGCCG 2: GGTTGTCTGGTAAAAGGACA
gRNA-(0-1)	pAC-U61-SapI	1: AGATCCAGCCAATCCCCCCG 2: AACAAGCTCCTTTAGACCCG
gRNA-(0-2)	pAC-U61-SapI	1: TTTCATACTCAACCTCGCCA 2: AACAAGCTCCTTTAGACCCG
gRNA-(0-3)	pAC-U61-SapI	1: TCGCAGAGCTGCATTAACCA 2: AACAAGCTCCTTTAGACCCG
gRNA-(0-4)	pAC-U61-SapI	1: GCTTCCCGAAGGGAGAAAGG 2: AACAAGCTCCTTTAGACCCG
gRNA-(0-5)	pAC-U61-SapI	1: CAAAAGCTGGAGCTCCACCG 2: AACAAGCTCCTTTAGACCCG
gRNA-(0-6)	pAC-U61-SapI	1: AATCACCTGCCAATAACTAG 2: AACAAGCTCCTTTAGACCCG
gRNA-Ptp69D	pAC-U61-SapI-Rev	1: CTAAGCGTGGTGATTCCCTG 2: GTTAAGGGATAAAAGAAACG 3: GAAGTTCCTGAAGTCTGCCG
gRNA-Nsf1	pAC-U63-tgRNA-Rev	1: AAAACGGTGGAGGTGCCCAG 2: GATGCCATTTGCAAGCAGCG
gRNA-Nsf2	pAC-U63-tgRNA-Rev	1: GAATGTGTCCGATTTCACGG 2: CCGCATCCTCGGTAACACGG
gRNA-Nsf1-Nsf2	pAC-U63-tgRNA-Rev	1: AAAACGGTGGAGGTGCCCAG 2: GATGCCATTTGCAAGCAGCG 3: GAATGTGTCCGATTTCACGG 4: CCGCATCCTCGGTAACACGG
gRNA-Snap24	pAC-U63-tgRNA-Rev	1: CCTCATGGACGAAAGCAAGG 2: ATTGATGAGCGGGAACGCGG
gRNA-Snap25	pAC-U63-tgRNA-Rev	1: CTCGGTCTTCGGGACCTGAG 2: GTAGCCCTTGATGATCAAGG
gRNA-Snap29	pAC-U63-tgRNA-Rev	1: GATGGATGACGATGACGAAG 2: TCTGCTCTACGAAACCCAGG
gRNA-Snap24-Snap25	pAC-U63-tgRNA-Rev	1: CCTCATGGACGAAAGCAAGG 2: ATTGATGAGCGGGAACGCGG 3: CTCGGTCTTCGGGACCTGAG 4: GTAGCCCTTGATGATCAAGG
gRNA-Snap24-Snap25-Snap29	pAC-U63-tgRNA-Rev	1: CCTCATGGACGAAAGCAAGG 2: ATTGATGAGCGGGAACGCGG 3: CTCGGTCTTCGGGACCTGAG 4: GTAGCCCTTGATGATCAAGG 5: GATGGATGACGATGACGAAG 6: TCTGCTCTACGAAACCCAGG

Table S4. Primer designs for cloning gRNA expression constructs.

Primer pair	Sequence	Note for $(N)_{20}$	PCR template
I. To make U6:1-gRNA1-U6:3-gRNA2 (w pAC-U61-SapI, pAC-U61-SapI-Rev, or pAC-U61-SapI-In)			
Primer pair 1 forward	agatatccgggtgaacttcG**(N)$_{20}$**GTTTTAGAGCTAGAAATAGCAAG	target sequence 1	pTGC-U63
Primer pair 1 reverse	gctatttctagctctaaaac**(N)$_{20}$**CGACGTTAAATTGAAAATAGG	target sequence 2, Rev Comp	
II. To make U6:1-gRNA1-U6:2-gRNA2-U6:3-gRNA3 (w pAC-U61-SapI, pAC-U61-SapI-Rev, or pAC-U61-SapI-In)			
Primer pair 1 forward	agatatccgggtgaacttcG**(N)$_{20}$**GTTTTAGAGCTAGAAATAGCAAG	target sequence 1	pTGC-U62
Primer pair 1 reverse	**(N)$_{20}$**CGAAGTATTGAGGAAAACATAC	target sequence 2, Rev Comp	
Primer pair 2 forward	**(N)$_{20}$**GTTTTAGAGCTAGAAATAGCAAG	target sequence 2	pTGC-U63
Primer pair 2 reverse	gctatttctagctctaaaac**(N)$_{20}$**CGACGTTAAATTGAAAATAGG	target sequence 3, Rev Comp	
III. To make dual tRNA-gRNA constructs (w pAC-U63-tgRNA-Rev)			
Primer pair 1 forward	TTCCCGGCCGATGCA**(N)$_{20}$**GTTTaAGAGCTAtgctgGAAAcag	target sequence 1	pMGC
Primer pair 1 reverse	TTCcagcaTAGCTCTtAAAC**(N)$_{20}$**TGCACCAGCCGGGAATC	target sequence 2, Rev Comp	
IV. To make quadruple tRNA-gRNA constructs (w pAC-U63-tgRNA-Rev)			
Primer pair 1 forward	TTCCCGGCCGATGCA**(N)$_{20}$**GTTTaAGAGCTAtgctgGAAAcag	target sequence 1	pMGC
Primer pair 1 reverse	**(N)$_{20}$**TGCACCAGCCGGGAATC	target sequence 2, Rev Comp	
Primer pair 2 forward	**(N)$_{20}$**GTTTaAGAGCTAtgctgGAAAcag	target sequence 2	pMGC
Primer pair 2 reverse	**(N)$_{20}$**TGCACCAGCCGGGAATC	target sequence 3, Rev Comp	
Primer pair 3 forward	**(N)$_{20}$**GTTTaAGAGCTAtgctgGAAAcag	target sequence 3	pMGC
Primer pair 3 reverse	TTCcagcaTAGCTCTtAAAC**(N)$_{20}$**TGCACCAGCCGGGAATC	target sequence 4, Rev Comp	

METHODS

Fly Stocks

ppk-Gal4 (HAN *et al.* 2012), *UAS-CD4-tdTom* (HAN *et al.* 2011), *UAS-CD4-tdGFP* (HAN *et al.* 2011), *UAS-Cas9* (PORT *et al.* 2014), *UAS-Dcr-2* (DIETZL *et al.* 2007), *ppk-CD4-tdGFP* (HAN *et al.* 2011), *tub-Gal80* (LEE AND LUO 1999), *tubP-Gal4 UAS-CD8-GFP* (LEE AND LUO 1999), *Gal4*$^{21\text{-}7}$ (SONG *et al.* 2007), *gRNA-e* (PORT *et al.* 2014) have been described previously. *Act-Gal4* (#3954), *UAS-GFP* (#6658), *UAS-mCherryNLS* (#38425), *UAS-RedStinger* (#8547), *nsyb-Gal4* (#39171), *Act-Cas9 w lig4* (#58492), *R28E04-Gal4* (#45169), Nrg-GFP (#6844) were obtained from Bloomington Stock Center (BDSC). *ppk-Cas9*, *RluA1-Cas9*, *SOP-Cas9*, *hh-Cas9*, *nsyb-tdGFP*, and various gRNA lines were made in this study.

To compare different gRNA-GFP designs, the strain *w; RluA1-Cas9; nsyb-GAL4 UAS-CD8-GFP* were crossed to various gRNA-GFP lines. To visualize large DNA deletions in individual neurons, *y Act5C-Cas9 w; nsyb-tdGFP*^{VK37} and *y Act5C-Cas9 w; nsyb-tdGFP*^{VK33} were crossed to various gRNA lines. *gRNA-Gal80* was used as *gRNA-0*.

Cas9-LEThAL assay

Act-Cas9 w lig4 homozygous females were crossed to *gRNA* homozygous males. The crosses were transferred several times to collect embryos in plastic vials on standard media. The embryo density was controlled at around 100 embryos per vial. The vials were monitored daily and animal lethal phases were recorded. If animals could pupariate, we counted the numbers of dead prepupae (before head eversion), dead pupae (post head eversion), dead pharate adults, and eclosed adults. For each lethal phase, we counted at least 100 animals for each cross.

Molecular Cloning

pDEST-APIC-Cas9: A synthetic core promotor containing Hsp70 core promoter, Inr, MTE, and DPE was synthesized as a gBlock fragment (Integrated DNA Technologies, Inc.) and was used to replace the Hsp70 core promoter of pDEST-HemmarR (HAN *et al.* 2011). The CD4-tdTom coding sequence of the resulting plasmid was then replaced with a fragment containing the *Streptococcus pyogenes* Cas9 coding sequence and two in-frame nuclear localization signals at both N- and C-termini of Cas9, which was amplified by PCR from pnos-Cas9 (REN *et al.* 2013) (a gift from Norbert Perrimon).

Enhancer entry vectors: pENTR-ppk was previously described (HAN *et al.* 2011). The R28E04 enhancer was PCR amplified from R28E04-Gal4 genomic DNA and was combined with pDONR221 (Thermo Fisher Scientific) to make pENTR-hh through a Gateway BP reaction. The pENTR-RluA1 was made

similarly using a 3.2 kb RluA1 enhancer that was PCR amplified from w^{1118} genomic DNA. The SOP enhancer contains 8 copies of *sc*-E1 element (POWELL *et al.* 2004) and was cloned into SalI/XhoI sites of pENTR11 (Thermo Fisher Scientific).

Cas9 expression vectors: ppk-Cas9, RluA1-Cas9, SOP-Cas9, hh-Cas9 expression vectors were generated by Gateway LR reactions using the appropriate entry vectors and a Cas9 destination vector which is similar to pDEST-APIC-Cas9 but does not contain Inr, MTE, and DPE in the Hsp70 core promoter.

nsyb-tdGFP: pAPIC-CD4-tdGFP (HAN *et al.* 2011) was digested by SphI and BamHI and assembled with a nsyb enhancer fragment, which was PCR-amplified from *R57C10-Gal4* genomic DNA, and a Hsp70 core promoter-intron fragment using NEBuilder DNA Assembly (New England Biolabs).

gRNA cloning vectors: Four gRNA cloning vectors were made using a pAC (attB-CaSpeR4) vector derived from pCaSpR4 (THUMMEL AND PIRROTTA 1992). pCFD4-U61-U63(PORT *et al.* 2014) was first digested by BbsI and then ligated with a SapI adapter made with annealed complementary oligos. A BglII-XbaI fragment from the resulting plasmid was isolated and cloned into BamHI/XbaI sites of pAC to make pAC-U61-SapI (i.e. Forward). An SpeI-XbaI fragment containing U6:1 promoter, SapI adapter, gRNA scaffold, and U6 3' flanking sequence was then isolated from pAC-U61-SapI and ligated back to SpeI/XbaI digested pAC-U61-SapI in the reverse orientation to make pAC-U61-SapI-Rev (i.e. Reverse). A Gypsy insulator fragment was PCR amplified from pEDST-HemmarR (HAN *et al.* 2011) and cloned into EcoR/SpeI sites of pAC-U61-SapI to make pAC-U61-SapI-In (i.e. Insulated). To make pAC-U63-tgRNA-Rev (i.e. tgFE), a DNA fragment containing *Drosophila* Gly tRNA, SapI adapter, the (F+E) gRNA scaffold, and U6 3' flanking sequence was synthesized as a gBlock (Integrated DNA Technologies, Inc.) and assembled with SapI/XbaI digested pAC-U63-SapI using NEBuilder DNA Assembly. The resulting plasmid was then digested by XbaI/SpeI, followed by re-ligation of the insert and the backbone in the reversed orientation.

gRNA PCR template vectors: Three PCR template vectors were made for generating PCR fragments used for assembling the final gRNA expression vectors. pTGC-U62 and pTGC-U63 are for cloning up to 3 gRNAs driven by separate U6 promotors in one construct (in Forward, Reverse, or Insulated design). pMGC is for making multiplex tRNA-gRNA vectors using the tgFE design. Each of these vectors were made by assembling a synthetic gBlock DNA fragment with a PCR-amplified Kanamycin-resistant backbone using NEBuilder DNA Assembly. The region to be PCR-amplified from pTGC-U62 contains the conventional gRNA scaffold, PolIII transcription terminator, and U6:2 promotor (PORT *et*

al. 2014). The region to be PCR-amplified from pTGC-U63 contains the conventional gRNA scaffold, PolIII transcription terminator, and U6:3 promotor (PORT *et al.* 2014). The region to be PCR-amplified from pMGC contains the (F+E) gRNA scaffold (CHEN *et al.* 2013) and rice Gly tRNA(PORT AND BULLOCK 2016).

Cloning of gRNA expression vectors: Primers were designed according to Table S4 and used to generate PCR products with the appropriate gRNA PCR template vectors. The PCR products were then assembled with SapI-digested gRNA cloning vectors using NEBuilder DNA Assembly (New England Biolabs Inc., #E2621). To make 2-4 gRNAs in one transgenic construct using the tgFE design, refer to Part III and IV of Table S4. More gRNAs can be added by increasing the number of PCR fragments similar to the second PCR fragment of Part IV. Purification of PCR fragments with commercial kits is recommended for assembling more than 4 gRNAs. Assembling >6 gRNAs in one assembly reaction is possible but has not been tested.

***Drosophila* Transgenic Lines**

Injections were carried out by Rainbow Transgenic Flies. Cas9 expression vectors were transformed using P-element-mediated random insertions. *nsyb-tdGFP* was generated by ΦC31-mediated integration at $attP^{VK37}$ and $attP^{VK33}$ sites. Unless noted otherwise, gRNA expression vectors were integrated into the $attP^{VK27}$ site.

Western blotting

NT2 (Table S1) males were crossed to either w^{1118} or *Act-Cas9* females. The embryos were collected overnight and allowed to develop to wandering third instar larvae. Animals of correct genotypes were then washed and collected in Eppendorf tubes and were frozen immediately on dry ice. Equal volumes of protein sample buffer (150 mM Tris.HCl pH 6.8, 7 M urea, 10% SDS, 24% glycerol, bromophenol blue) supplemented with 10% 2-mercaptoethanol was added and samples were homogenized using a pestle tissue grinder (VWR #47747-370). The samples were then centrifuged at the maximum speed in a tabletop centrifuge (Eppendorf Centrifuge 5424) for 10 minutes before the supernatants were transferred to clean tubes. The supernatants were then resolved on 10% SDS-polyacrylamide gels and then transferred to nitrocellulose blotting membranes (GE Healthcare Life Sciences). Antibodies to GFP (Torrey Pines Biolabs, rabbit, 1:10,000), mCherry (Abcam clone 1C51, mouse, 1:4000) and CD8 (Abcam, CD8-α [EPR21769], rabbit, 1:1000) were used for the primary binding. After incubation with secondary antibodies (IRDye 800CW Goat anti-Rabbit IgG and IRDye 680RD Goat anti-Mouse IgG, 1:10,000 for each), the proteins were visualized using Li-Cor system. Westernblot experiments were

performed at least three times from four biological replicates. The Western band intensities were measured in Fiji using Gels functions.

Identification of gRNA target sequence

We used two gRNA prediction tools, sgRNA Scorer 2.0(CHARI *et al.* 2017) (https://crispr.med.harvard.edu) and Benchling (www.benchling.com), to identify candidate gRNA target sequences that have high on-target scores in both algorithms. Target sequences predicted to have more than one target site by CasFinder (AACH *et al.* 2014) were rejected. For each gene, we selected two target sequences that are against coding exons of all splicing isoforms. We prefer to use target sequences in the common coding exons of the first half of the gene. All targeting sequences designed by this study are listed in Table S3.

Live Imaging

Snapshot live imaging of larval da neurons was performed as described previously (POE *et al.* 2017). Briefly, animals were reared at 25°C in density-controlled vials. Third instar larvae at 96 hr AEL (unless specified otherwise) were mounted in glycerol and imaged with a Leica SP8 confocal. For dendritic phenotypes, the A2-A3 segments of 8-10 larvae were imaged for each genotype using a 20X oil objective. For all other experiments, the A1-A4 segments of 5-6 larvae were imaged for each genotype using a 40X oil objective. To image larvae younger than 72 hr AEL, larvae were anesthetized by isoflurane for 2 minutes & then mounted in halocarbon oil.

To image day 0 adults, the wings of newly eclosed male and female flies were removed. A thin layer of vacuum grease was placed on a glass slide and flies were then mounted with the dorsal side pressed into the grease. A small amount of UV glue (glue NOA61; Norland) was then added to the ventral side of the animal (about 0.1 μL) and a coverslip was placed on top of the animals and pressed slightly. Then, the glue was cured by UV light (a modified version of WorkStar 2003 NDT 365 nm UV-A Inspection Light) at Hi setting for 30 seconds. V'ada neurons of the abdominal segments were then imaged using a 40X oil objective.

Imaginal disc imaging

Dissection of imaginal discs was performed as described previously (HAN *et al.* 2004). Briefly, wandering 3rd instar larvae were dissected in a small petri dish filled with PBS. The anterior half of the larva was inverted and the trachea and gut were removed. The sample was then transferred to 4% formaldehyde in PBS and fixed for 15 minutes at room temperature. After washing with PBS, the

imaginal discs were placed in SlowFade Diamond Antifade Mountant (Thermo Fisher Scientific) on a glass slide. A coverslip was slightly pressed on top and the discs were imaged using a 40X oil objective.

Immunohistochemistry

Antibodies used in this study are mouse anti-Cas9 (Novus, 1:500) and rabbit anti-dNSF (1:5000) (YU *et al.* 2011). Secondary antibodies conjugated to DyLight dyes (Jackson ImmunoResearch) were used at 1:500 dilution. Immunostaining of *Drosophila* larvae was performed as described previously (POE *et al.* 2017). Briefly, 3rd instar larvae were dissected in cold PBS, fixed in 4% formaldehyde/PBS for 20 min at room temperature, and stained with the proper primary antibodies and subsequent secondary antibodies, overnight at 4 °C for primary antibodies and for 2 hr at room temperature for secondary antibodies.

Image analysis and quantification

Tracing and measuring of C4da dendrites was performed as described previously (POE *et al.* 2017). Briefly, for tracing and measuring C4da dendrites (Figure 4G, Figure 5, and Figure 6) in Fiji/ImageJ, images of dendrites (1,024 X 1,024 pixels) taken with a 20X objective were first processed by Gaussian Blur (Sigma: 0.8) and then Auto Local Threshold (Phansalkar method, radius: 50). Isolated particles below the size of 120 pixels were removed by the Particles4 plugin (http://www.mecourse.com/landinig/software/software.html). The dendrites were then converted to single-pixel-width skeletons using the Skeletonize (2D/3D) plugin and processed using Analyze Skeleton (2D/3D) plugin. The length of skeletons was calculated based on pixel distance; terminal dendrites in the dendritic field or regions of interest were counted based on the endings of terminal dendrites. Skeletons of terminal dendrites in regions of interest were isolated using the Strahler Analysis plugin (http://imagej.net/Strahler_Analysis). Dendrite density was calculated using the formula: 1000 X dendritic length (μm)/dendritic area (μm^2); normalized terminal dendrite number was calculated using the formula: 1000 X terminal dendrite number/dendritic area (μm^2).

The GFP fluorescence intensity of neurons were measured in Fiji/ImageJ (Figure 1, Figure 2, and Figure 4). Z-stack images were taken for each dorsal sensory cluster with a 40X oil objective. The slice with the brightest and most uniform GFP signal at the cell body and primary dendrites of the neuron of interest was identified and a region of interest (ROI) was defined at the cell body or primary dendrites. For experiments involving negative testers, regions overlapping with neuronal nuclei were not included in the ROIs in order to avoid potential blead-through from the RFP channel. To identify cell bodies that had very weak fluorescence, the images were first brightened up using the Brightness/Contrast tool.

To count GFP-positive neurons in Figure 3, each slice in image stacks was inspected and all visible cell bodies were counted as GFP-positive neurons. The identities of missing PNS neurons were estimated based on relative cell body locations in the PNS dorsal cluster.

Statistical Analysis

R was used to perform one-way analysis of variance (ANOVA) with Tukey's HSD test for most experiments (unless specified otherwise). Excel was used to perform Student's t-test where indicated.

SUPPLEMENTAL REFERENCE

Aach, J., P. Mali and G. M. Church, 2014 CasFinder: Flexible algorithm for identifying specific Cas9 targets in genomes. bioRxiv.

Chari, R., N. C. Yeo, A. Chavez and G. M. Church, 2017 sgRNA Scorer 2.0: A Species-Independent Model To Predict CRISPR/Cas9 Activity. ACS Synth Biol 6**:** 902-904.

Chen, B., L. A. Gilbert, B. A. Cimini, J. Schnitzbauer, W. Zhang *et al.*, 2013 Dynamic imaging of genomic loci in living human cells by an optimized CRISPR/Cas system. Cell 155**:** 1479-1491.

Desai, C., and J. Purdy, 2003 The neural receptor protein tyrosine phosphatase DPTP69D is required during periods of axon outgrowth in Drosophila. Genetics 164**:** 575-588.

Dietzl, G., D. Chen, F. Schnorrer, K. C. Su, Y. Barinova *et al.*, 2007 A genome-wide transgenic RNAi library for conditional gene inactivation in Drosophila. Nature 448**:** 151-156.

Golby, J. A., L. A. Tolar and L. Pallanck, 2001 Partitioning of N-ethylmaleimide-sensitive fusion (NSF) protein function in Drosophila melanogaster: dNSF1 is required in the nervous system, and dNSF2 is required in mesoderm. Genetics 158**:** 265-278.

Han, C., T. Y. Belenkaya, B. Wang and X. Lin, 2004 Drosophila glypicans control the cell-to-cell movement of Hedgehog by a dynamin-independent process. Development 131**:** 601-611.

Han, C., L. Y. Jan and Y. N. Jan, 2011 Enhancer-driven membrane markers for analysis of nonautonomous mechanisms reveal neuron-glia interactions in Drosophila. Proc Natl Acad Sci U S A 108**:** 9673-9678.

Han, C., D. Wang, P. Soba, S. Zhu, X. Lin *et al.*, 2012 Integrins regulate repulsion-mediated dendritic patterning of drosophila sensory neurons by restricting dendrites in a 2D space. Neuron 73**:** 64-78.

Lee, T., and L. Luo, 1999 Mosaic analysis with a repressible cell marker for studies of gene function in neuronal morphogenesis. Neuron 22**:** 451-461.

Morelli, E., P. Ginefra, V. Mastrodonato, G. V. Beznoussenko, T. E. Rusten *et al.*, 2014 Multiple functions of the SNARE protein Snap29 in autophagy, endocytic, and exocytic trafficking during epithelial formation in Drosophila. Autophagy 10**:** 2251-2268.

Poe, A. R., L. Tang, B. Wang, Y. Li, M. L. Sapar *et al.*, 2017 Dendritic space-filling requires a neuronal type-specific extracellular permissive signal in Drosophila. Proc Natl Acad Sci U S A 114**:** E8062-E8071.

Port, F., and S. L. Bullock, 2016 Augmenting CRISPR applications in Drosophila with tRNA-flanked sgRNAs. Nat Methods 13**:** 852-854.

Port, F., H. M. Chen, T. Lee and S. L. Bullock, 2014 Optimized CRISPR/Cas tools for efficient germline and somatic genome engineering in Drosophila. Proc Natl Acad Sci U S A 111**:** E2967-2976.

Powell, L. M., P. I. Zur Lage, D. R. Prentice, B. Senthinathan and A. P. Jarman, 2004 The proneural proteins Atonal and Scute regulate neural target genes through different E-box binding sites. Mol Cell Biol 24**:** 9517-9526.

Ren, X., J. Sun, B. E. Housden, Y. Hu, C. Roesel *et al.*, 2013 Optimized gene editing technology for Drosophila melanogaster using germ line-specific Cas9. Proc Natl Acad Sci U S A 110**:** 19012-19017.

Royou, A., M. E. Gagou, R. Karess and W. Sullivan, 2010 BubR1- and Polo-coated DNA tethers facilitate poleward segregation of acentric chromatids. Cell 140**:** 235-245.

Song, W., M. Onishi, L. Y. Jan and Y. N. Jan, 2007 Peripheral multidendritic sensory neurons are necessary for rhythmic locomotion behavior in Drosophila larvae. Proc Natl Acad Sci U S A 104**:** 5199-5204.

Thummel, C. S., and V. Pirrotta, 1992 New pCaSpeR P-element vectors. Drosophila Inf. Serv. 71**:** 150.

Vilinsky, I., B. A. Stewart, J. Drummond, I. Robinson and D. L. Deitcher, 2002 A Drosophila SNAP-25 null mutant reveals context-dependent redundancy with SNAP-24 in neurotransmission. Genetics 162**:** 259-271.

Yu, W., F. Kawasaki and R. W. Ordway, 2011 Activity-dependent interactions of NSF and SNAP at living synapses. Mol Cell Neurosci 47**:** 19-27.